# Reliability estimation of underground fuel tank limit states

Przemysław SORN[1,2], Mateusz SONDEJ[1], and Jarosław GÓRSKI[1]*

[1] Faculty of Civil and Environmental Engineering, Gdańsk University of Technology, Poland
[2] KB Pomorze, Gdańsk, Poland

**Abstract.** Fuel tanks are designed with regard to standard loads and operating conditions. The investigations of the paper show the impact of such factors as tank corrosion and other means on the variation of stress fields and deformation of the underground horizontal tank shell. The introduction of probabilistic methods allows for structural reliability assessment. While the computational time of the entire tank FEM model is high, the preliminary analysis is restricted to the structural part only. The analysis makes it possible to optimize the structure with regard to construction costs.

**Key words:** underground fuel tanks; shell corrosion; reliability analysis.

## 1. INTRODUCTION

Pressure tanks are structures requiring high responsibility in the current design. The possible effects of failure are financial losses related to the loss of stored material, a break in the technological process, or tank reconstruction. Tank failures are also associated with a risk to human health and life. Pollution of both the natural environment and groundwater brings enormous consequences, too.

The regulations currently introduced in the European Union in the form of the PED directive [1] require that the essential safety demands are met as specified in Annex I to Directive 2014/68/EU. In terms of design, the directive presents general directions in the selection of a computational method, without providing a detailed approach. To ensure compliance of the pressure equipment design, e.g., tanks with the PED directive [1], the designer may apply a set of standards adjusted with the regulation, e.g., EN13445 [2] or standards that guarantee compliance with the requirements of the directive, e.g., the Terms of the Office of Technical Inspection (WUDT) or the ASME Boiler and Pressure Vessel Code. It is assumed that meeting relevant criteria of load capacity and serviceability as well as appropriately selected design standard-based solutions will ensure an appropriate level of safety and durability. However, none of the studies specifies how the level of safety is measured in a quantitative mode.

The statement above may be responded to by full or partial application of the standard provisions of the Eurocode series, particularly PN-EN 1990 Eurocode [3] and PN-EN 1993-4-2 Eurocode 3 [4]. The PN-EN 1990 [3] standard addresses the safety of a structure in terms of its reliability, and consequently introduces the reliability index $\beta$. This indicator is affected by the class of consequences CC1, CC2, and CC3. The standard assumes that the computations are carried out based on partial safety factors, which allows us to directly estimate the reliability index $\beta$ and to compare it with its limit value given in Table B2 PN-EN 1990 [3].

In addition, the Eurocode series qualify liquid gas tanks for the CC3 consequence class. The reference period of 50 years, the pressure vessels reliability index $\beta$ is 4.3, which corresponds to the probability of failure $p_f$ lower than 0.00001 [1,2]. It seems reasonable to measure the reliability of tanks designed according to standards not related to the Eurocode series (e.g., [5]). A comparison of the different design methods was made, for example, in [6].

The FE models of fuel tanks should exceed the deterministic analytical standards for perfect structures, to consider the issues like material and geometric imperfections and post-welding stresses [7]. The influence of the interaction between the tank and the subsoil cannot be neglected either [8]. Due to the random nature of tank data, probabilistic methods are commonly used. A review of the methods allowing us to estimate the structural reliability (SRA) and the stochastic finite element method (SFEM), covering both technological and application issues, is presented, e.g., in [9]. The problem of determining the limit values of the parameters of imperfections and their impact on the stress/strain state of a shell structure is the subject of numerous papers, e.g., [10, 11]. Reliability assessment is incorporated to address the impact of corrosion-based degradation [12, 13].

Commercial engineering software allows us to perform linear bifurcation analysis (LBA) and geometrically and materially non-linear analysis (GMNA) [14]. While the tanks are often loaded by negative pressure, it is essential to consider imperfections during analysis, i.e., geometrically non-linear analysis of imperfect structures (GNIA) or geometrically and physically non-linear analysis of imperfect structures (GMNIA).

*e-mail: jgorski@pg.edu.pl

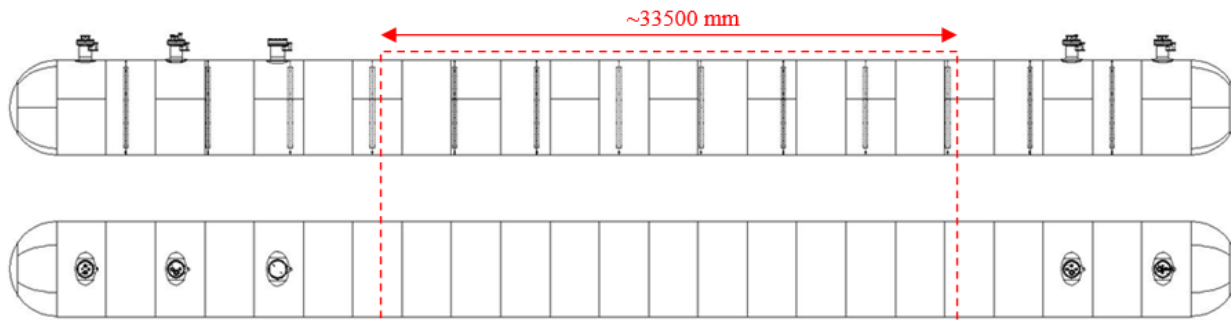*Bull. Pol. Acad. Sci. Tech. Sci.*, vol. 71, no. 2, p. e144588, 2023

1

**Fig. 1.** The analysed underground fuel storage tank

The work presents a preliminary analysis of a simplified model of an underground fuel tank. Some parameters are selected, e.g., softening (thickness reduction) of sheets due to corrosion and the number of stiffeners, and a check is completed of their impact on critical states due to negative pressure.

A simplified reliability assessment of the tank is performed, indicating a broad safety margin of a structure designed according to Eurocode standards. Custom computations facilitate the optimization of the structure and achievement of its required consequence class (CC3). The work contributes to the formulation of these types of non-standard computational algorithms. The implementation of innovative calculation methods in practice plays a major role where the safety and long-term reliability of structures is required [15].

## 2. THE TANK FEM MODEL

The analysis concerns a standard underground storage horizontal tank. The tank length is 72599 mm, outer diameter is 5600 mm (Fig. 1). The base material applied for tank manufacture is steel P355NL2, 28 mm thick for the cylindrical shell and 26 mm thick for the hemispherical ends. The cylindrical shell is stiffened with 13 T-shaped rings. The tank features five manholes in the upper region.

First of all preliminary analysis is completed with regard to the simplified tank models (Fig. 2). The computations are performed for the cylindrical shell of the following parameters: length $L$33500 mm (half of the real tank length) and diameter $d_c = 5600$ mm (Fig. 1). The computations are conducted using the ABAQUS software [14]. The model incorporates 37632 shell elements. Simplified boundary conditions are represented by restrained translations at both edges. This modelling pattern of boundary conditions is possible because of specific loading, i.e., negative pressure. The edges of a simplified tank model are stiffened (Fig. 1), it is possible to represent them by restraints at all nodes. Negative pressure was assumed at its initial value of $p = 1.0$ MPa. The negative pressure multiplier $p$ is investigated to yield global or local stability loss. The computations are directed to the corrosion check by means of sheet thickness reduction in the case of overall or partial tank analysis. The impact of stiffener spacing is investigated too.

The following variants of tank loading are assumed (Fig. 3):
1. Internal radial pressure $p_n$

2. Compressive load in the longitudinal direction, the derivative of internal pressure $p_x$
3. The combination of internal radial pressure $p_n$ and compressive load in longitudinal direction $p_x$
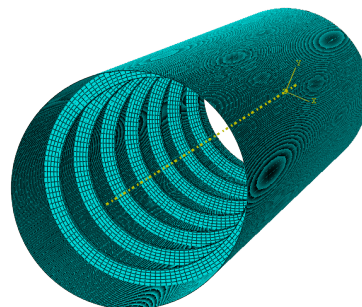


**Fig. 2.** Simplified models of an underground fuel tank including stiffening ribs (ABAQUS [14])
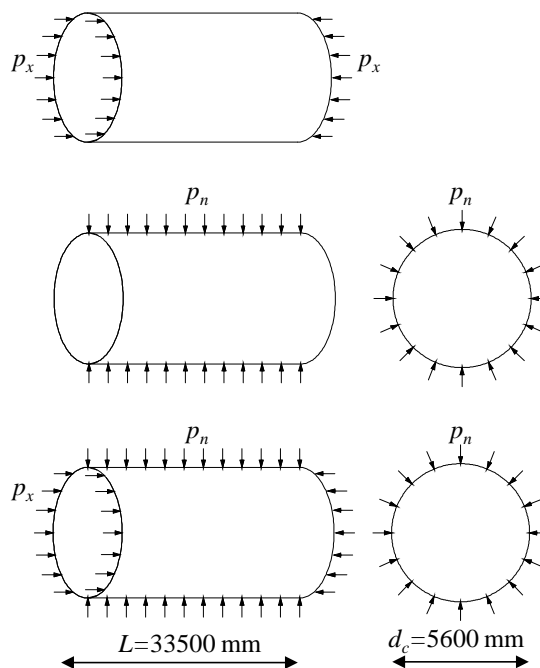


$L=33500$ mm    $d_c=5600$ mm

**Fig. 3.** Tank load cases

2

*Bull. Pol. Acad. Sci. Tech. Sci.*, vol. 71, no. 2, p. e144588, 2023

The longitudinal load $p_x$ is a function of radial load $p_n$:

$$\pi R^2 p_n = 2\pi R p_x \quad \rightarrow \quad p_x = 1400 p_n, \qquad (1)$$

where $R$ is the tank radius.

## 3. THE RESULTS OF THE PRELIMINARY ANALYSIS

The following computational variants were conducted:

1. Unstiffened cylindrical shell of uniform thickness – the impact of overall tank thickness variation on buckling
2. Unstiffened cylindrical shell of a constant basic thickness equal $t = 28$ mm, and locally reduced thickness along the generating line (the reduced strip is denoted by the angle $\alpha = 30, 90, 180$ [deg])
3. Stiffened cylindrical shell with a variable number of stiffeners ($n_s = 1, 2, 3, 6$)

Figures 4 and 5 compare the critical pressure results with regard to variable sheet thickness $t$ and two different loading schemes. The variation of sheet thickness $t$ reflects the corrosion processes which may happen in a long-term tank operation. It was assumed that the reduction of sheet thickness is uniform throughout the entire shell. A high impact was observed of longitudinal load $p_x$ (Fig. 4), radial load $p_n$, and the combination of both $p_n$ and $p_x$ (Fig. 5). A 20% critical pressure drop is observed in the combination case of $p_n$ and $p_x$. The deformed form of the tank (ABAQUS [14]) is presented in Fig. 6. The computations proved the necessity to consider these loads in the analysis of pressure tanks.
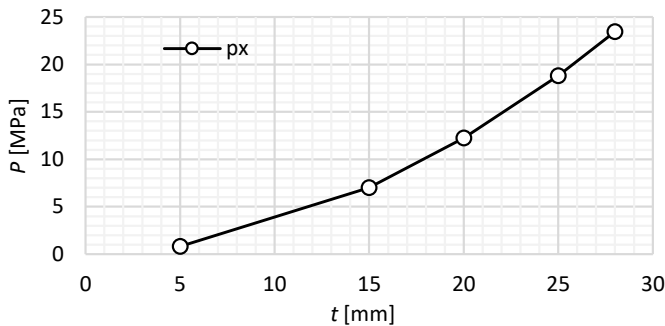


**Fig. 6.** Buckling modes of an unstiffened tank loaded with the combination of external pressure $p_n$ and longitudinal pressure $p_x$ (ABAQUS [14])

The second analyzed model considers local corrosion. The wall thickness reduction along the circumference is defined by the angle $\alpha$ (Fig. 7). The tank is loaded by a combination of external pressure $p_n$ and longitudinal pressure $p_x$.



**Fig. 7.** Illustration of the assumed shell part of reduced sheet thickness (the impact of the corrosion process)

Figure 8 presents the effect of angle range and thickness reduction on the tank's critical pressure. The buckling modes of an unstiffened tank with partially reduced thickness are presented in Fig. 9.

The third computational series is intended to check the number of stiffeners preventing the tank from buckling. The ring stiffener spacing is essential for optimal tank design. Figure 10



**Fig. 4.** Unstiffened cylindrical shell with uniform thickness: the impact of sheet thickness $t$ on critical pressure $p_x$
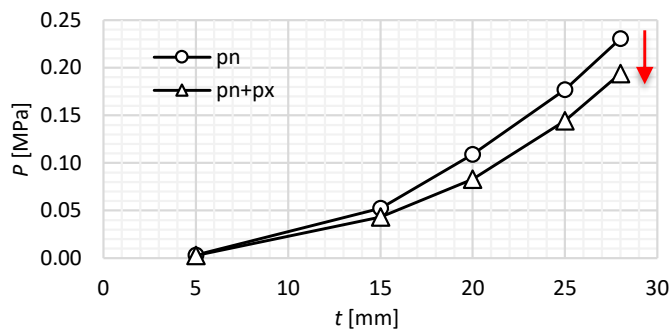


**Fig. 5.** Unstiffened cylindrical shell with uniform thickness: the impact of sheet thickness $t$ on critical pressure $p_x$ and the combination of both $p_n$ and $p_x$
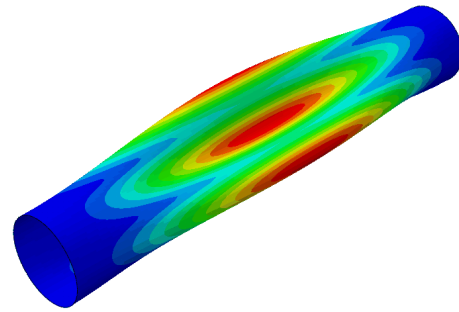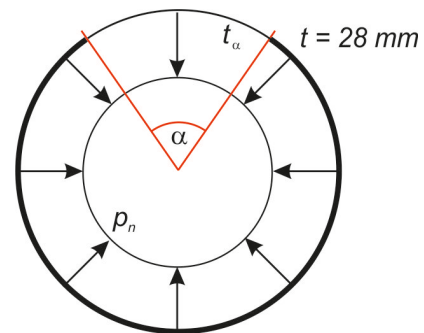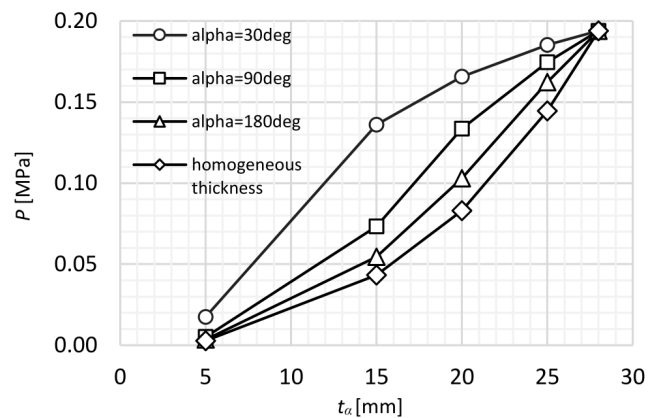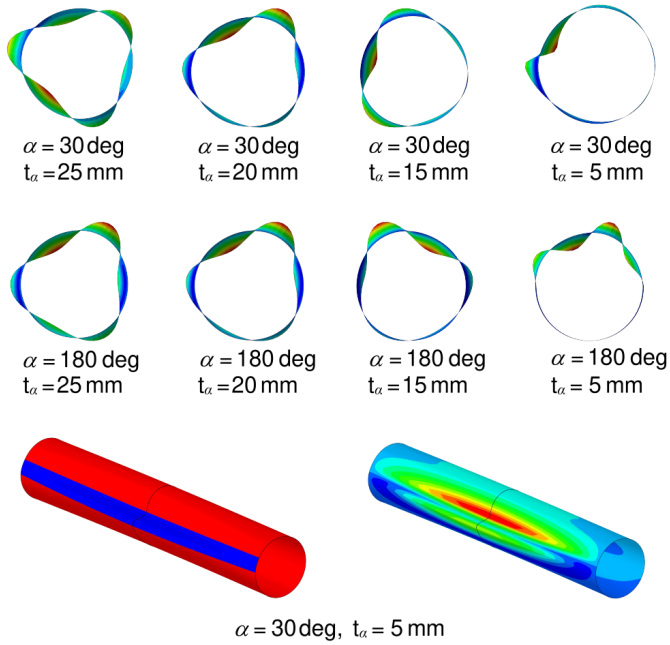


**Fig. 8.** Unstiffened cylindrical shell with partially reduced thickness – the impact of range and thickness reduction on the critical load

*Bull. Pol. Acad. Sci. Tech. Sci.*, vol. 71, no. 2, p. e144588, 2023

3

$\alpha = 30\,\mathrm{deg}$
$t_\alpha = 25\,\mathrm{mm}$

$\alpha = 30\,\mathrm{deg}$
$t_\alpha = 20\,\mathrm{mm}$

$\alpha = 30\,\mathrm{deg}$
$t_\alpha = 15\,\mathrm{mm}$

$\alpha = 30\,\mathrm{deg}$
$t_\alpha = 5\,\mathrm{mm}$

$\alpha = 180\,\mathrm{deg}$
$t_\alpha = 25\,\mathrm{mm}$

$\alpha = 180\,\mathrm{deg}$
$t_\alpha = 20\,\mathrm{mm}$

$\alpha = 180\,\mathrm{deg}$
$t_\alpha = 15\,\mathrm{mm}$

$\alpha = 180\,\mathrm{deg}$
$t_\alpha = 5\,\mathrm{mm}$

$\alpha = 30\,\mathrm{deg}, \; t_\alpha = 5\,\mathrm{mm}$

**Fig. 9.** Buckling modes of an unstiffened tank with partially reduced thickness

shows the impact of the number of stiffeners on the critical load (LBA) in the case of longitudinal $p_x$ and normal $p_n$ pressure.
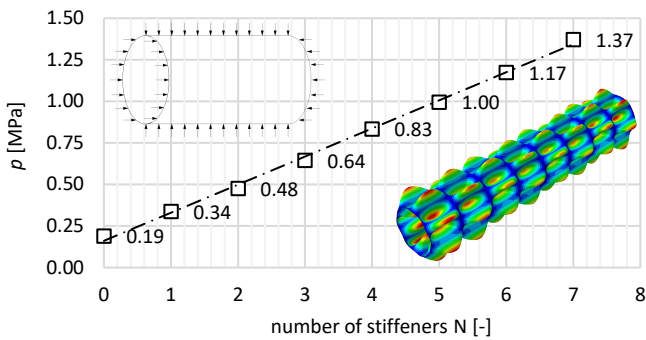


**Fig. 10.** Critical load of the stiffened cylindrical shell subjected to longitudinal compressive load and external pressure related to the number of stiffeners

The computational results presented in Fig. 10 allow us to conclude the following:

- In the case of internal negative pressure, a 700% increase in critical load was observed for the tank with seven rings compared to the unstiffened one.
- The ring stiffeners increase the critical load in a linear mode.
- Buckling waves occur between the ring stiffeners.
- The number of buckling waves in circumferential depends on the number of stiffeners number, it is constant in longitudinal directions (always a single half-wave between the rings).

The last stage of the preliminary analysis is aimed at comparing the design critical stresses of the stiffened cylindrical shell

subjected to a longitudinal compressive force (Fig. 11). The following conclusions are drawn:

- The critical load of the unstiffened tank is slightly lower than the classical critical pressure $\left(\sigma_{\mathrm{cr}} = 0.605 E \dfrac{t}{r}\right)$.
- In the case of tanks with four or a greater number of stiffeners, the difference between classical critical pressure and the FE results is less than 5%.
- An 8% increase in critical pressure is observed between the model with seven stiffeners and the unstiffened one.
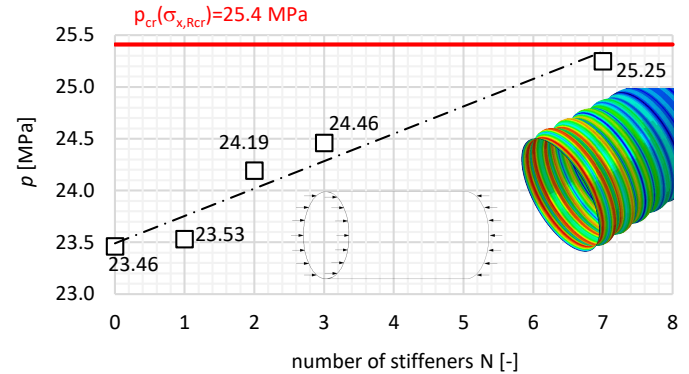


**Fig. 11.** Critical load of the stiffened cylindrical shell subjected to longitudinal compressive load related to the number of stiffeners

## 4. AN INQUIRY DIRECTED TO SHELL THICKNESS ACCORDING TO CODES

One of the first computational steps in tank design is aimed at determining the shell wall thickness of the overpressure tank. For this purpose, the EN13445-3 standard [2] specifies maximum allowable stresses for the tank operation phase and during pressure testing. With regard to tanks made of carbon steel, allowable stresses may be specified according to points 6.2 or 6.3 (Table 6.1, EN13445-3 [2]):

$$\text{point 6.2:} \quad f_{d(6.2)} = \min\left(\frac{R_{p0.2/T}}{1.5}; \; \frac{R_{m/20}}{2.4}\right), \qquad (2)$$

$$\text{point 6.3:} \quad f_{d(6.3)} = \min\left(\frac{R_{p0.2/T}}{1.5}; \; \frac{R_{m/20}}{1.875}\right). \qquad (3)$$

For the design variant corresponding to the pressure test concerning points 6.2 and 6.3, the expressions are identical (compare equations (2) and (3)). On the other hand, in the design variant corresponding to the operation phase of the tank, the expressions differ in the range of the applied reduction coefficients of the tensile strength ($R_m$). As a result, in the case of calculations according to point 6.3, the allowable stresses are higher than in the case of calculations based on point 6.2, which consequently leads to lower shell thickness. A graphical image of these relations is schematically shown in Fig. 12.

According to EN 1990 [3], storage pressure vessels should be assigned to the CC2 consequence class due to the consequences of destruction, in specific cases (storage of energy media of strategic importance for the state energy policy), CC3 class. These consequence classes are directly correlated with
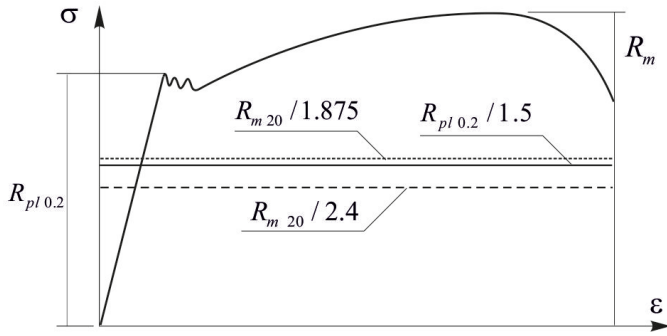
4

*Bull. Pol. Acad. Sci. Tech. Sci.*, vol. 71, no. 2, p. e144588, 2023

**Fig. 12.** Steel stress diagram

the RC2 and RC3 reliability classes (Table B1, EN1990 [3]) corresponding to the minimum values of the reliability index, equal to 4.3 and 3.8 in the 50 years (Table B2, EN1990 [3]).

Calculations conducted in accordance with EN1993-1-6 [4] and the calculation factors given in EC0 lead to the designed structure meeting the requirements for the RC2 reliability class and achieving a minimum reliability factor of 3.8 in the 50 years. It should be noted that calculations according to the limit state design do not state the reliability index directly but it is only assumed that the minimum requirements shown in table B2 of EN1990 [3] are met. Moreover, the designed structures classified as CC3 and RC3 require the designer to prove that they meet the minimum requirements of the reliability index at the level of 4.3 without providing the method or guidelines to assess the actual reliability index.

Figure 13 shows the computational results of the shell wall thickness for the operating stage according to points 6.2 and 6.3 (EN13445-3 standard [2]) the design variant for the pressure test according to EN13445-3 [2] and for the operating stage according to EN1993-1-6 [4] using the limit state design method with standard values of calculation factors allowing us to presume compliance at the minimum reliability index level of $\beta = 3.8$.
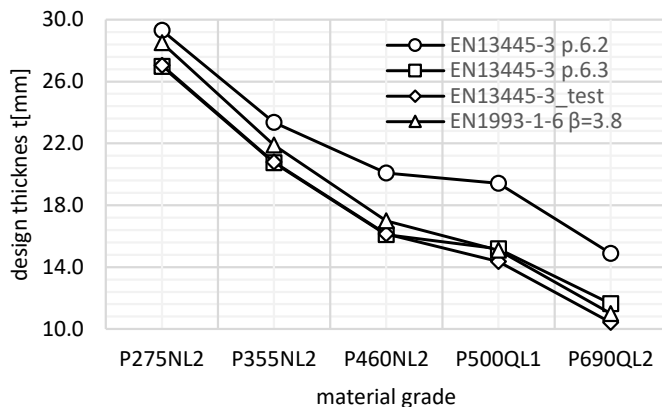


**Fig. 13.** Shell wall thickness according to points 6.2 and 6.3 (EN13445-3)

Analysis of the results (Fig. 13) leads to the conclusion that the calculations according to point 6.2 result in the thickness of the shell wall being very high compared to the calcula-

tions made according to point 6.3 and in accordance with EC3. It should be noted that the structure designed in accordance with EC3 meets the assumptions of the minimum required reliability index at the level of 3.8. Therefore, it is doubtful if the computations made in accordance with point 6.2 significantly increase structural reliability with a significant increase in financial outlays.

## 5. TANK RELIABILITY ESTIMATIONS

Determining the actual reliability level of the designed tanks requires the adoption of appropriate random variables of yield strength of steel and shell thickness. The yield strength $R_e$ is assigned a Gaussian variable, its parameters are based on laboratory tests:

$$R_e = N(371.00,\ 7.05)\ [\text{MPa}]. \tag{4}$$

The shell thickness $t$ is also linked with a normal variable whose parameters are based on literature data [16]:

$$t = N(23.98,\ 0.77)\ [\text{mm}]. \tag{5}$$

The limit state $G(R_e, t)$ is reached while the shell structure undergoes stress equal to the yield strength under the pressure $p$:

$$G(R_e, t) = R_e - \sigma = R_e - \frac{pr}{t}. \tag{6}$$

Substituting the value of the tank radius $r = 2800$ mm and the pressure $p = 1.71$ MPa adopted as deterministic parameters, the expression (6) takes the following form:

$$G(R_e, t) = R_e - \frac{4788}{t}. \tag{7}$$

To assess structural reliability the functions (7) are expanded into the Taylor series:

$$G(R_e, t) \approx G(\bar{R}_e, \bar{t}) + \frac{\partial G}{\partial R_e}(R_e - \bar{R}_e) + \frac{\partial G}{\partial t}(t - \bar{t}). \tag{8}$$

Performing subsequent operations:

$$\frac{\partial G}{\partial R_e} = 1, \quad \frac{\partial G}{\partial t} = \frac{4788}{t^2} = \frac{4788}{23.98^2} = 8.33 \tag{9}$$

the limit stare function may be determined as follows:

$$G(R_e, t) \approx 171.3 + (R_e - 371.0) + 8.33(t - 23.98). \tag{10}$$

Applying (10) $R_e = \bar{R}_e$ and $t = \bar{t}$ the mean value is $\bar{G}(R_e, t) = 171.3$ MPa. The variance of the function $G(R_e, t)$ follows the standard formula, applying $\sigma_{R_e} = 7.05$ MPa and $\sigma_t = 0.77$ mm:

$$\sigma_G^2 \approx (1.0\sigma_{R_e})^2 + (8.33\sigma_t)^2 = 90.4\ \text{MPa}^2. \tag{11}$$

Finally, the standard deviation of the limit state function equals $\sigma_G = 9.51$ MPa. The determined values make it possible

*Bull. Pol. Acad. Sci. Tech. Sci.*, vol. 71, no. 2, p. e144588, 2023

5

to assess the reliability:

$$P_f = P(G < 0) = \Phi\left(\frac{0 - \overline{G}}{\sigma_G}\right) = \Phi(-18.01) \simeq 0.0, \quad (12)$$

where the function is the cumulative distribution function of the standard Gaussian variable.

Due to formula (12), the reliability index is $\beta = 18.01$.

Table 1 summarizes the results of computations carried out for tanks of variable nominal thickness:

- 28 mm – the real tank – thickness introduced in the computations $t = 24.7$ mm (the calculated thickness is the result of subtracting corrosion allowance and negative deviation of geometric tolerance).
- Design thickness determined by the values of allowable stresses in accordance with point 6.2 of EN13445-3 (2) – $t = 23.35$ mm.
- Design thickness determined by the values of allowable stresses in accordance with point 6.3 of EN13445-3 (3) – $t = 20.74$ mm.

**Table 1**
Tank reliability calculations depending on the shell thickness

| Parameter | The real tank | Calculated thickness EN13445-3 point 6.2 | Calculated thickness EN13445-3 point 6.3 |
|---|---|---|---|
| Nominal thickness [mm] | 24.70 | 23.35 | 20.74 |
| Mean value $G(R_e,t)$ [MPa] | 171.30 | 160.00 | 134.00 |
| Variance $G(R_e,t)$ [MPa$^2$] | 90.40 | 95.13 | 107.31 |
| Standard deviation $G(R_e,t)$ | 9.508 | 9.75 | 10.36 |
| Failure probability $p_f$ [%] | $\approx 0$ | $\approx 0$ | $\approx 0$ |
| Index $\beta$ [–] | 18.01 | 16.41 | 12.93 |

The results are also shown in Figs. 14 and 15. The analysis shows that the limit state is not exceeded in any case, the esti-
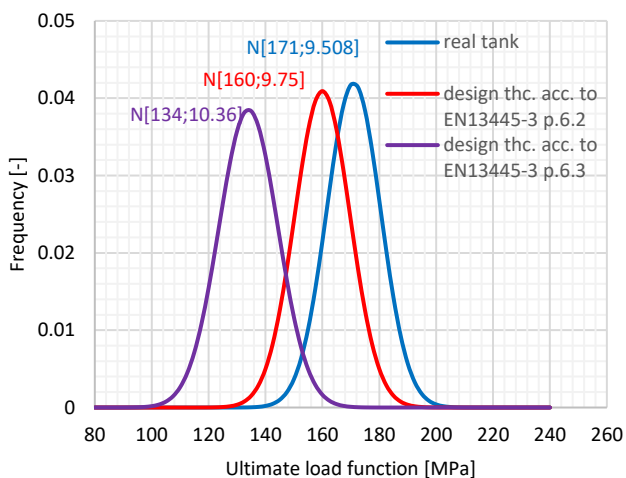


**Fig. 14.** Probability density function for pressure vessel under internal pressure

mated reliability indices are much higher values than the values provided in the standards.
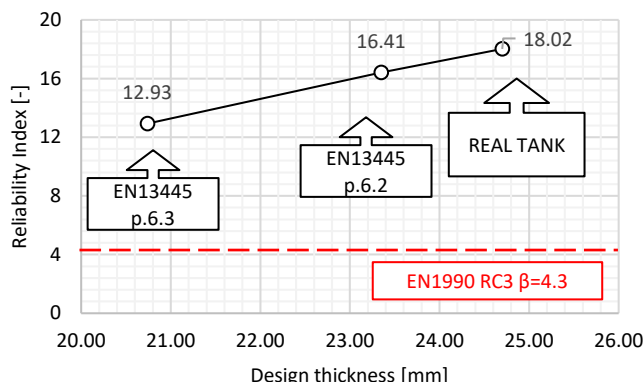


**Fig. 15.** Reliability index of pressure vessel ultimate limit state function – internal pressure

The analysis is also carried out to assess the probability of reaching allowable stresses within the structure, in accordance with points 6.2 (2) and 6.3 (3) of EN13445-3 [2] for steel of P355NL2 grade:

$$f_{d6.2} = 204.17 \text{ MPa}, \quad (13)$$

$$f_{d6.3} = 236.67 \text{ MPa}. \quad (14)$$

The stresses are defined by a function of a random variable, expressed by the equation:

$$\sigma(t) = \frac{pr}{t} = \frac{4788}{t}. \quad (15)$$

Applying the Taylor series expansion (8), after relevant computations, standard deviations and mean values of the stress function are determined for tanks of a variable nominal thickness (Table 2). The probability of exceeding allowable stresses is estimated according to points 6.2 and 6.3 of EN13445-3 [2]. The results are presented graphically in Fig. 16.
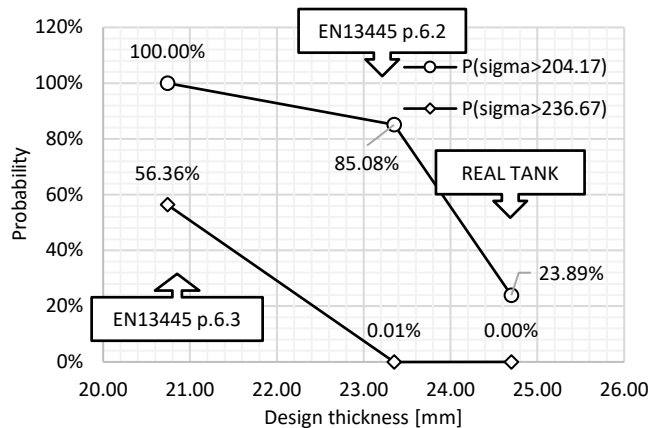


**Fig. 16.** Probability of exceeding the permissible stresses in pressure tank shell under internal pressure

6

*Bull. Pol. Acad. Sci. Tech. Sci.*, vol. 71, no. 2, p. e144588, 2023

#### Table 2
Tank reliability calculations

| Parameter | The real tank | Calculated thickness EN13445-3 point 6.2 | Calculated thickness EN13445-3 point 6.3 |
|---|---|---|---|
| Nominal thickness [mm] | 24.70 | 23.35 | 20.74 |
| Mean walue $G(R_e,t)$ [MPa] | 199.70 | 211.2 | 237.85 |
| Variance $G(R_e,t)$ [MPa$^2$] | 40.68 | 45.53 | 57.58 |
| Standard deviation $G(R_e,t)$ [MPa] | 6.378 | 6.748 | 7.588 |
| Failure probability $p_f > f_{6.2}$ [%] | 23.89 | 85.08 | 99.99956 |
| Failure probability $p_f > f_{6.3}$ [%] | $\approx 0$ | 0.007841 | 56.36 |

## 6. CONCLUSIONS

Preliminary underground tank analysis proved the following:
- Variation in tank thickness decreases the negative pressure bringing stability loss.
- Local reduction of shell thickness yields the reduction of negative pressure causing stability loss.
- While the difference between the nominal shell thickness and its reduced value is substantial, local stability loss occurs in the reduced thickness region.
- The use of reinforcing stiffeners of appropriately high stiffness increases the cylinder load-carrying capacity, and the required negative pressure to yield stability loss is higher than the value related to the unstiffened shell.
- The obtained reliability indices are several times (3–4) greater than the required reliability index level specified by the EC0 standard.
- Within the boundary state, i.e., achieving the stresses equal to the yield strength, analysis of the values of the reliability indices makes it possible to optimize the shell thickness by up to 4 mm.

The conducted computations and further conclusions are bound to accelerate the computations in the complex FEM model. The results of numerical calculations should also be verified by measurements made on real objects or by laboratory tests, e.g., [17].

## ACKNOWLEDGEMENTS

## REFERENCES

[1] Directive 2014/68/EU of the European Parliament and of the Council of 15 May 2014 on the harmonisation of the laws of the Member States relating to the making available on the market of pressure equipment.

[2] Non-flame-heated pressure tanks Part 3. Design, EN 13445-3.

[3] Eurocode – Fundamentals of structural design, EN 1990.

[4] Eurocode 3 – Design of steel structures part 4-2. Tanks, EN 1993-6.

[5] M. Kamiński and P. Świta, "Structural stability and reliability of the underground steel tanks with the Stochastic Finite Element Method," *Arch. Civil Mech.l Eng.,* vol. 15, pp. 593–602, 2015, doi: 10.1016/j.acme.2014.04.010.

[6] E. Azzuni and S. Guzey, "Comparison of the shell design methods for cylindrical liquid storage tanks," *Eng. Struct.*, vol. 101, pp. 621–630, 2015, doi: 10.1016/j.engstruct.2015.07.050.

[7] K. Rasiulis, A. Šapalas, R. Vadlūga, and M. Samofalov, "Stress/strain state investigations for extreme points of thin wall cylindrical tanks," *J. Constr. Steel. Res.*, vol. 62, pp. 1232–1237, 2006, doi: 10.1016/j.jcsr.2006.04.016.

[8] P.M. Lewiński, "Accuracy assessment of linear elasticity solution for interaction of cylindrical tank with subsoil" *Bull. Polish Acad. Sci. Tech. Sci.*, vol. 69, no. 1 p. e136039, 2021, doi: 10.24425/bpasts.2021.136039.

[9] M. Aldosary, J. Wang, and C. Li, "Structural reliability and stochastic finite element methods: State-of-the-art review and evidence-based comparison," *Eng. Comput.*, vol. 35, pp. 2165–2214, 2018, doi: 10.1108/EC-04-2018-0157.

[10] J.M. Rotter, "Shell buckling design and assessment and the LBA-MNA methodology," *Stahlbau*, vol. 80, no. 11, pp. 791–803, 2011, doi: 10.1002/stab.201101491.

[11] J. Górski, T. Mikulski, M. Oziębło, and K. Winkelman, "Effect of geometric imperfections on aluminium silo capacities," *Stahlbau*, vol. 84, no. 1, pp. 52–57, 2015, doi: 10.1002/stab.201510224.

[12] W. Geary and J. Hobbs, "Catastrophic failure of a carbon steel storage tank due to internal corrosion," *Case Stud. Eng. Fail. Anal.*, vol. 1, pp. 257–264, 2013, doi: 1016/j.csefa.2013.09.002.

[13] R.E. Melchers, "Estimating uncertainty in maximum pit depth from limited observational data," *Corros. Eng. Sci. Technol.*, vol. 45, no 3, pp. 240–248, 2010, doi: 10.1179/147842209X12489567719581.

[14] M. Smith, ABAQUS/Standard User's Manual, Version 6.9, Dassault Systèmes Simulia Corp, Providence, RI 2009

[15] L. Czarnecki and D. Van Gemert, "Innovation in construction materials engineering versus sustainable development," *Bull. Polish Acad. Sci. Tech. Sci.*, vol. 65, no. 6, pp. 765–771, 2017, doi: 10.1515/bpasts-2017-0083.

[16] A. Biegus, *Probabilistic analysis of steel structures*, Warszawa, Wrocław: Scientific Publisher PWN 1999 (in Polish).

[17] W. Buczkowski, A. Szymczak-Graczyk, and Z. Walczak, "Experimental validation of numerical static calculations for a monolithic rectangular tank with walls of trapezoidal cross-section," *Bull. Polish Acad. Sci. Tech. Sci.*, vol. 65, no. 6, pp. 799–804, 2017, doi: 10.1515/bpasts-2017-0088.